Final Performance Report – Years 1-3

Project Title:	*Innervated Blood-Brain-Barrier Tissue for the Study of Neuroinvasion by VEEV*
Award Number:	N00173-16-2-C007
Reporting Period:	12/07/2015 - 7/06/2018
Program Manager:	Dr. Russell K. Pirlo/Code 6115 Naval Research Laboratory 4555 Overlook Avenue SW Washington, D.C. 20375 E-mail: russell.pirlo@nrl.navy.mil
Principal Investigator:	Professor Charles M. Lieber Department of Chemistry and Chemical Biology Harvard University 12 Oxford Street Cambridge, MA 02138 E-mail: cml@cmliris.harvard.edu Phone: (617) 496-3169

REPORT DOCUMENTATION PAGE

Form Approved
OMB No. 0704-0188

PLEASE DO NOT RETURN YOUR FORM TO THE ABOVE ADDRESS.

1. REPORT DATE *(DD-MM-YYYY)*	2. REPORT TYPE	3. DATES COVERED *(From - To)*
28-09-2018	Final	12/07/2015 - 7/06/2018

4. TITLE AND SUBTITLE

Innervated Blood-Brain-Barrier Tissue for the Study of Neuroinvasion by VEEV

5a. CONTRACT NUMBER

5b. GRANT NUMBER

N00173-16-2-C007

5c. PROGRAM ELEMENT NUMBER

6. AUTHOR(S)

Lieber, Charles M.

5d. PROJECT NUMBER

5e. TASK NUMBER

5f. WORK UNIT NUMBER

7. PERFORMING ORGANIZATION NAME(S) AND ADDRESS(ES)

President and Fellows of Harvard College
Richard A. and Susan F. Smith Campus Center
1350 Massachusetts Avenue, Suite 600
Cambridge, MA 02138-3846

8. PERFORMING ORGANIZATION REPORT NUMBER

9. SPONSORING/MONITORING AGENCY NAME(S) AND ADDRESS(ES)

Naval Research Laboratory
ATTN: Code 5596
4555 Overlook Avenue SW
Washington, D.C. 20375

10. SPONSOR/MONITOR'S ACRONYM(S)

11. SPONSOR/MONITOR'S REPORT NUMBER(S)

12. DISTRIBUTION/AVAILABILITY STATEMENT

Approved for public release, distribution unlimited

13. SUPPLEMENTARY NOTES

14. ABSTRACT

With the goal of understanding how Venezuelan equine encephalitis virus (VEEV) infection permeates the blood-brain barrier (BBB), this collaborative project seeks to develop a BBB tissue model that can eliminate many of the shortcomings of current methods to map viral transport and host response in real time by use of an innovative 3D tissue model based on flexible nanoscale field-effect transistor (FET) technology developed in our laboratory. We supported the project's goal of elucidating VEEV pathogenesis by developing, testing and providing to NRL, with appropriate training, nanoFET mesh arrays and measurement systems to develop the BBB model. We also developed sensing strategies based on chemical functionalization of mesh arrays for specific antigen detection in physiological solutions using VEEV analogues.

15. SUBJECT TERMS

blood-brain barrier, innervated tissue model, nanoscale field-effect transistor, VEEV, viral pathogenesis

16. SECURITY CLASSIFICATION OF:			17. LIMITATION OF ABSTRACT	18. NUMBER OF PAGES	19a. NAME OF RESPONSIBLE PERSON
a. REPORT	b. ABSTRACT	c. THIS PAGE			Charles M. Lieber
U	U	U	UU	14	19b. TELEPHONE NUMBER *(Include area code)* 617-496-3169

Reset

INSTRUCTIONS FOR COMPLETING SF 298

1. REPORT DATE. Full publication date, including day, month, if available. Must cite at least the year and be Year 2000 compliant, e.g. 30-06-1998; xx-06-1998; xx-xx-1998.

2. REPORT TYPE. State the type of report, such as final, technical, interim, memorandum, master's thesis, progress, quarterly, research, special, group study, etc.

3. DATES COVERED. Indicate the time during which the work was performed and the report was written, e.g., Jun 1997 - Jun 1998; 1-10 Jun 1996; May - Nov 1998; Nov 1998.

4. TITLE. Enter title and subtitle with volume number and part number, if applicable. On classified documents, enter the title classification in parentheses.

5a. CONTRACT NUMBER. Enter all contract numbers as they appear in the report, e.g. F33615-86-C-5169.

5b. GRANT NUMBER. Enter all grant numbers as they appear in the report, e.g. AFOSR-82-1234.

5c. PROGRAM ELEMENT NUMBER. Enter all program element numbers as they appear in the report, e.g. 61101A.

5d. PROJECT NUMBER. Enter all project numbers as they appear in the report, e.g. 1F665702D1257; ILIR.

5e. TASK NUMBER. Enter all task numbers as they appear in the report, e.g. 05; RF0330201; T4112.

5f. WORK UNIT NUMBER. Enter all work unit numbers as they appear in the report, e.g. 001; AFAPL30480105.

6. AUTHOR(S). Enter name(s) of person(s) responsible for writing the report, performing the research, or credited with the content of the report. The form of entry is the last name, first name, middle initial, and additional qualifiers separated by commas, e.g. Smith, Richard, J, Jr.

7. PERFORMING ORGANIZATION NAME(S) AND ADDRESS(ES). Self-explanatory.

8. PERFORMING ORGANIZATION REPORT NUMBER. Enter all unique alphanumeric report numbers assigned by the performing organization, e.g. BRL-1234; AFWL-TR-85-4017-Vol-21-PT-2.

9. SPONSORING/MONITORING AGENCY NAME(S) AND ADDRESS(ES). Enter the name and address of the organization(s) financially responsible for and monitoring the work.

10. SPONSOR/MONITOR'S ACRONYM(S). Enter, if available, e.g. BRL, ARDEC, NADC.

11. SPONSOR/MONITOR'S REPORT NUMBER(S). Enter report number as assigned by the sponsoring/ monitoring agency, if available, e.g. BRL-TR-829; -215.

12. DISTRIBUTION/AVAILABILITY STATEMENT. Use agency-mandated availability statements to indicate the public availability or distribution limitations of the report. If additional limitations/ restrictions or special markings are indicated, follow agency authorization procedures, e.g. RD/FRD, PROPIN, ITAR, etc. Include copyright information.

13. SUPPLEMENTARY NOTES. Enter information not included elsewhere such as: prepared in cooperation with; translation of; report supersedes; old edition number, etc.

14. ABSTRACT. A brief (approximately 200 words) factual summary of the most significant information.

15. SUBJECT TERMS. Key words or phrases identifying major concepts in the report.

16. SECURITY CLASSIFICATION. Enter security classification in accordance with security classification regulations, e.g. U, C, S, etc. If this form contains classified information, stamp classification level on the top and bottom of this page.

17. LIMITATION OF ABSTRACT. This block must be completed to assign a distribution limitation to the abstract. Enter UU (Unclassified Unlimited) or SAR (Same as Report). An entry in this block is necessary if the abstract is to be limited.

Final Performance Report – Years 1-3

Background and Objectives. The blood-brain barrier (BBB) BBB is a specialized, selectively permeable seal which regulates diffusion of molecules and microorganisms from the blood to the brain. This barrier is essential to function of the central nervous system (CNS), enabling tight regulation of molecular transport and thereby protecting the brain from pathogenic organisms. However, in certain instances, this protective effect can be lost. A number of pathologies associated with CNS disease disrupt BBB permeability by, for instance, altering expression of pro-inflammatory cytokines. Venezuelan equine encephalitis virus (VEEV) is a mosquito-borne virus considered a potential biological warfare agent due to its high infectivity when aerosolized. VEEV is capable of crossing the BBB and damaging neuronal cells, and the host innate immune response may increase the permeability of the BBB and contribute to mortality. There is evidence that direct infection of the BBB by VEEV also plays an important role in pathogenesis. As such, there is a need for detailed analysis of how virus transport to the CNS occurs at the molecular level.

With the ultimate goal of understanding how VEEV infection permeates the BBB, this project led by Naval Research Laboratory (NRL) sought to develop a BBB tissue model that can eliminate many of the shortcomings of current methods to map viral transport and host response in real time. Their proposed 3D tissue model is based on flexible nanoscale field-effect transistor (FET) technology developed in our laboratory, folded and stacked to create a 3D innervated tissue, Flexible nanoFET arrays are an open-mesh network allowing true 3D connectivity of engineered tissue and 3D organization of sensory devices throughout tissue, and as such have advantages over traditional microelectrode arrays (MEAs) and patch clamps. Additionally, the mechanical properties of the nanoFET arrays are orders of magnitude softer than existing MEA structures and the energy required to bend elements in the scaffold is similar to cell-membrane deformation energy, heretofore unique for any electronics. These properties should therefore enable sustained monitoring at the BBB and eliminate necrosis and apoptosis often observed around traditional electrodes. By creating distributed nano-FETs capable of specific detection of VEEV, cell-signaling and other antiviral molecules, fluorescent labelling and gene transfection can be avoided, eliminating the need to sacrifice and section the tissue to achieve time course measurement. Our provision of these mesh arrays to NRL and their integration with Navy-patented layer-by-layer cell printing technology can enable creation of a unique innervated tissue model of the BBB with the ability to map host response and viral transport in real time during neuroinvasion by VEEV.

We supported the project's overall goal of elucidating pathogenesis of the VEEV disease model by pursuing the following objectives:

(1) Purchase, fabrication, assembly and testing of nanoFET array measurement systems for NRL/USAMRIID, and training in their use;

(2) Design, fabrication and characterization of nanoFET mesh arrays;

(3) Delivery of first-generation nanoFET mesh arrays to NRL for cell printing/tissue culture and subsequent monitoring of neuronal activity with embedded nanoFETs;

(4) Development of chemical functionalization of nanoFET mesh arrays for specific antigen detection, and testing and characterization of the functionalized arrays;

(5) Development of sensing strategy for specific detection of VEEV analogue dextran and VEEV-like particles in physiological solutions.

Work performed toward these objectives is described below:

<u>Objective 1.</u> Purchase, fabrication, assembly and testing of nanoFET mesh measurement systems for NRL and USAMRIID, and training in their use.

Silicon nanowire (SiNW) nanoFET mesh input/output interface design optimization. Components of two parallel measurement systems were purchased and assembled by our group according to detailed lists specified in the original cost proposal. To accommodate NRL's bioreactor designs, a reliable input/output (I/O) interface between SiNW nanoFET mesh and recording instrumentation was needed for high yield, low noise connections. Our group has actively developed and optimized I/O interface design, from first generation Si-wafer wire-bonding through second-generation Omnetics zero-insertion-force (ZIF) connectors and third-generation flat-flexible-cable (FFC)-ZIF connectors (**Figure 1**).

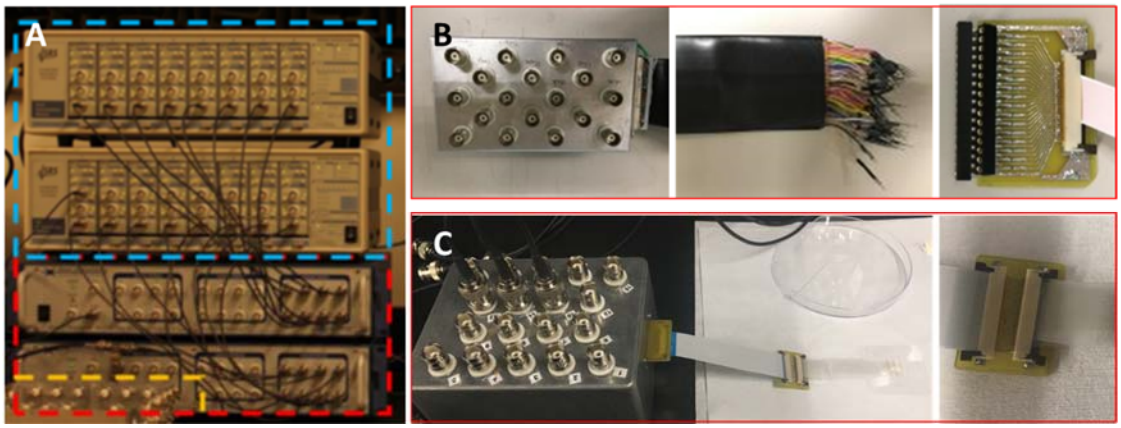

Figure 1. (A) Recording instrumentation set-up, including 16-channel current preamplifier (blue dashed box) and 16-channel analog signal digitizer (red dashed box). **(B)** Second generation of I/O interface design, with Omnetics ZIF connector. **(C)** Third generation of I/O interface design with FFC-ZIF-ZIF connector.

In addition, contact resistance measurements were carried out to investigate the connection quality of our interface designs. Utilization of a FFC-ZIF-ZIF interface enabled us to achieve a contact resistance of 608.6 ± 6.5 Ω, indicating excellent and uniform ohmic contact formation between channels (**Table 1**).

614	609	614	604
609	609	614	605
610	609	614	609
597	592	614	615

Table 1. Contact resistance measurements for each channel.

Training of NRL personnel and equipment transfer. Xiaochuan Duan, Dr. Teng Gao, and Dr. Jinlin Huang trained NRL personnel (Dr. Joel Gaston) on assembly of SiNW nanoFET mesh using ZIF connectors (**Figure 2**), and operation of the sensing instrumentation, including recording parameter settings and data acquisition and analysis. Following training, one of the measurement systems was transferred to NRL.

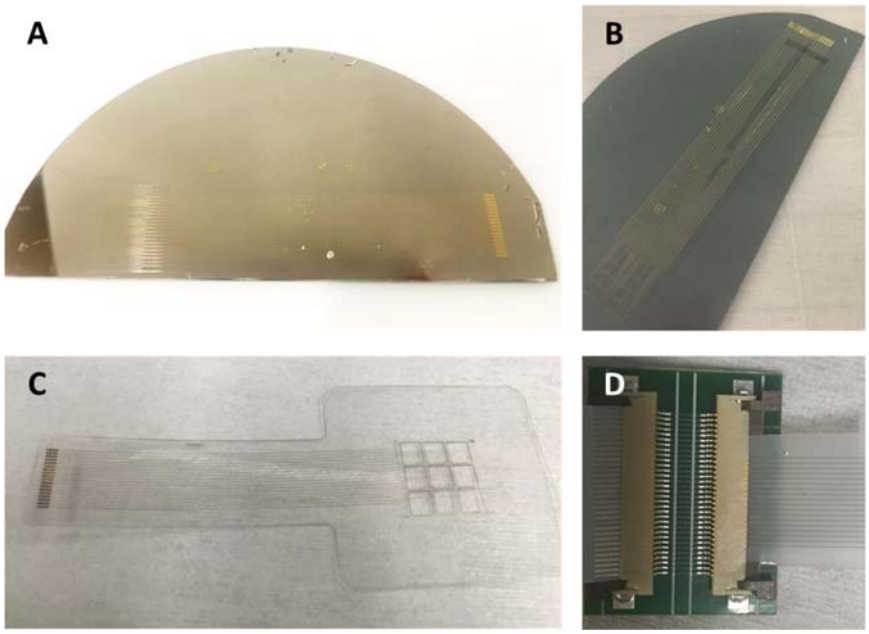

Figure 2. SiNW nanoFET assembly instructions. **(A)** Cut SiNW nanoFET mesh wafer in half. **(B)** Release mesh from wafer by etching of Ni sacrificial layer in Ni etchant TFB (Transene). **(C)** Transfer and align mesh onto the cyclic olefin copolymer (COC) substrate provided by NRL. **(D)** Insert and align mesh/COC complex in ZIF connector.

<u>Objective 2.</u> Design, fabrication and characterization of nanoFET mesh arrays.

Design and fabrication of nanoFET mesh arrays. Several SiNW nanoFET mesh designs were proposed for compatibility with NRL-designed bioreactor designs. We followed a SiNW nanoFET fabrication protocol developed by our group which consists of five main steps briefly listed below. The optimized design was finalized as shown in **Figure 3**. Two meshes were fabricated on a 3-inch Si wafer, with 16 SiNW nanoFET sensors located in a 4x4 array at the end of the mesh.

1. 100 nm sacrificial Ni layer deposition onto Si wafer by thermal evaporation.
2. Photolithography to define SU8 2000.5 photoresist islands for SiNW contact printing.
3. Photolithography to define and fabricate bottom SU8 2000.5 support layer.
4. Photolithography to define metal contacts patterns and I/O pads of the mesh, followed by 2 nm Cr/100 nm Au deposition by thermal evaporation.
5. Photolithography to define and fabricate the top SU8 2000.5 support layer.

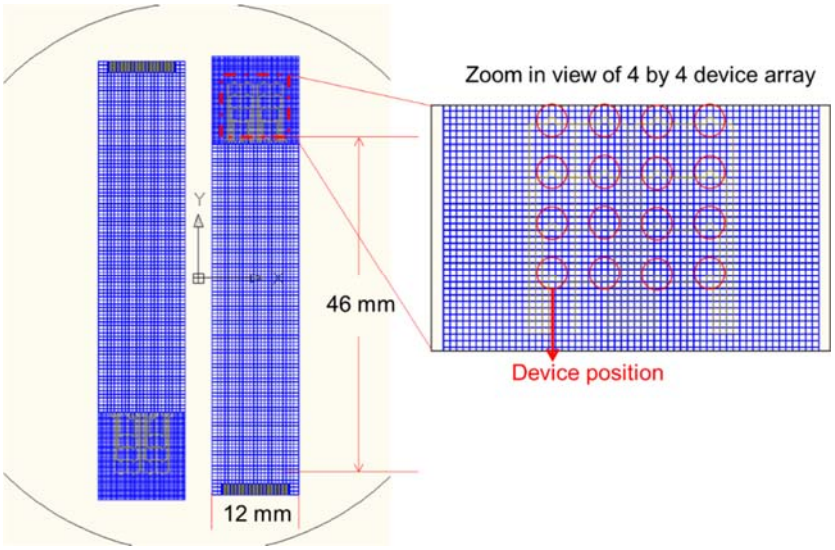

Figure 3. SiNW nanoFET mesh design and device position layout (labeled by red circle)

Characterization of nanoFET mesh arrays. Before SiNW nanoFET mesh delivery to NRL, SiNW FET characteristics were measured to evaluate device performance, including noise analysis, current-voltage transfer characteristic and water-gate performance assessment. With the optimized ZIF I/O interface, source-drain current (I_{ds})/source-drain voltage (V_{ds}) plots for five representative SiNW nanoFETs (**Figure 4A**) are linear, consistent with good ohmic contact. The corresponding noise level (**Figure 4B**) ranges from 20 to 100 nS (nanosiemens), similar to the noise level for on-chip SiNW FET sensors. Our fabricated SiNW FET sensors present typical p-doped field transistor characteristics in a water-gate response test in 1X phosphate-buffered saline (PBS) using gold wire as gate electrode, as seen in **Figure 5** with the noise power spectrum, and the relative signal-to-noise (SNR) is calculated as 530, 1480, 1410 and 840 V^{-1} based on the four water-gate response plots in **Figure 5A**. These characterizations demonstrate that the ZIF connectors enable a good and reliable I/O interface, and the SiNW FET sensors were deemed ready for delivery and modification.

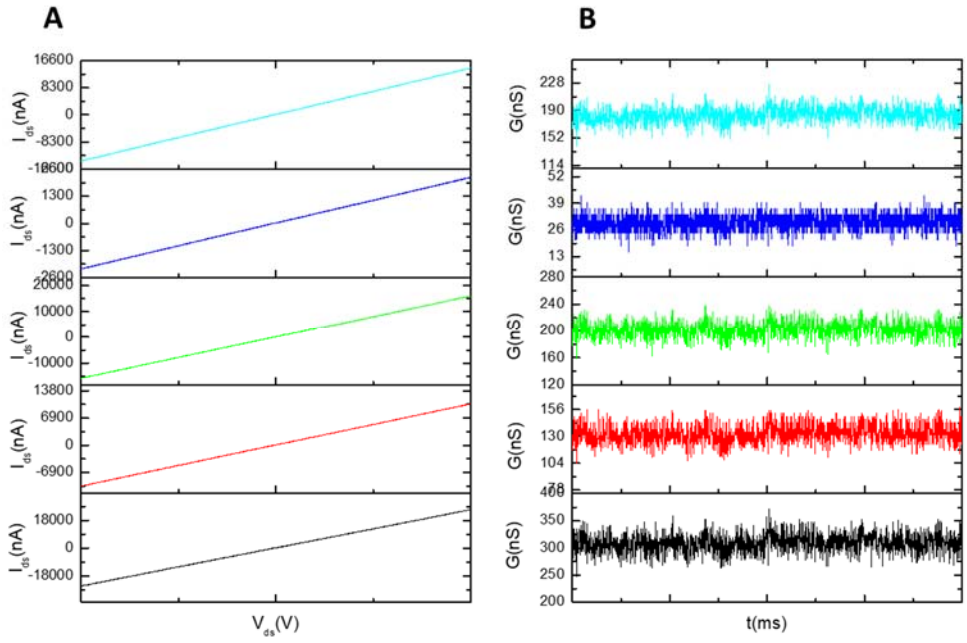

Figure 4. (A) I_{ds}-V_{ds} device characteristics of five representative SiNW nanoFETs. **(B)** 200 seconds of continuous recording of corresponding SiNW nanoFETs for analyzing noise level.

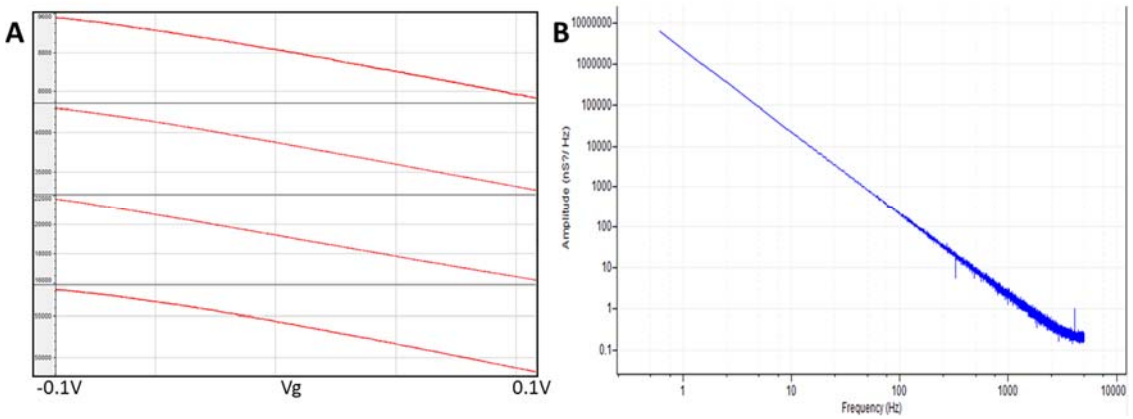

Figure 5. (A) Water-gate response test carried out on SiNW nanoFET sensors. **(B)** Noise-frequency power spectrum with 1 kHz digital low-pass filter.

Rhodamine labeled SiNW nanoFET mesh fabrication. We also fabricated rhodamine-labeled SiNW nanoFET meshes and sent them to NRL for cell culture imaging applications. The rhodamine labeling technique utilizes a crosslinking reaction between the primary amino group of rhodamine and residual epoxy groups from the SU-8 mesh frames. The confocal fluorescence microscopic image in **Figure 6** indicates stable and uniform rhodamine labeling across the mesh frames.

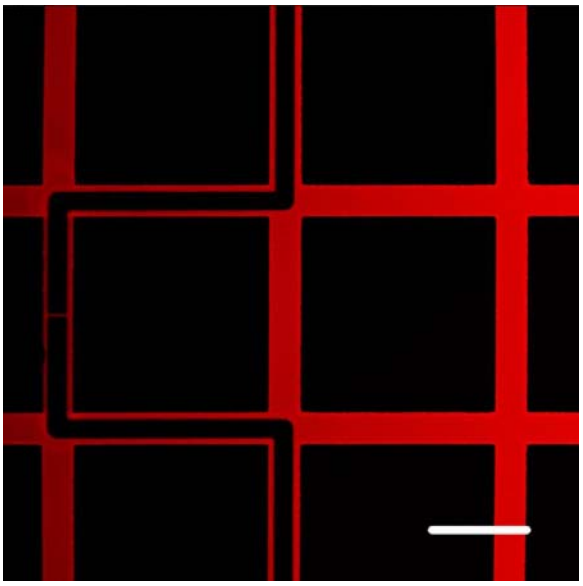

Figure 6. Confocal fluorescence microscopic image of rhodamine-labeled SiNW nanoFET mesh. (Scale bar = 100 μm)

We subsequently helped NRL determine the cause of photobleaching of the rhodamine-labeled mesh (UV sterilization) and recommended an alternate sterilization procedure that would not damage the rhodamine dye.

Objective 3. Delivery of first-generation nanoFET meshes to NRL for cell printing/tissue culture and subsequent monitoring of neuronal activity with embedded nanoFETs.

SiNW nanoFET meshes delivered to NRL. SiNW nanoFET meshes were first fabricated on Si wafer, then released and transferred to laser-cut COC substrate. Prior to shipping, the meshes were interfaced with ZIF connectors and tested to evaluate current-voltage characteristics of individual devices, prior to delivery. Delivery dates and pin assignments for each mesh are listed below:

Date	**Batch No.**	**Chip No.**	***Note***
2017.03.13	1	Chip2, Chip3	*Not glued*
2017.03.24	2	Chip5, Chip8	*Not glued*
2017.03.31	3	Chip7L, Chip5L	*Chip5L glued*
2017.04.14	4	Chip9L, Chip10L	*Chip10L glued*
2017.04.21	5	Chip11L, Chip11R	*Not glued*
2017.04.28	6	Chip10R, Chip12R	*Chip12R glued*
2017.05.15	7	Chip13L, Chip13R	*Not glued*
2017.05.22	8	Chip14L, Chip14R	*Not glued*
2017.06.05	9	R1, R2	*Rhodamine-labeled*
2017.06.03	10	Chip15L, Chip15R	*Not glued*
2017.06.20	11	Chip16L, Chip16R	*Not glued*
2017.07.17	12	Chip17L, Chip17R	*Not glued*
2017.07.26	13	Chip18L, Chip18R	*Not glued*

Table 2. Details of SiNW nanoFET mesh delivery to NRL

Figure 7. Detailed pin assignments for each SiNW nanoFET mesh device.

Packaging of nanoFET arrays for delivery. Due to the delicate connections within the mesh assemblies, the proportion of functioning pins in early shipments to NRL was lower than desired. We developed a packaging method to minimize device loss during shipping. The protocol involved reinforcing the connection of the ZIF connector to the mesh with epoxy glue, which resulted in a dramatic improvement in yield. For protection from static electricity build-up, the devices were shipped inside anti-static containers wrapped in aluminum foil and secured within the containers with copper tape (**Figure 8**). The containers were in turn immobilized in the shipping boxes with tightly packed bubble wrap.

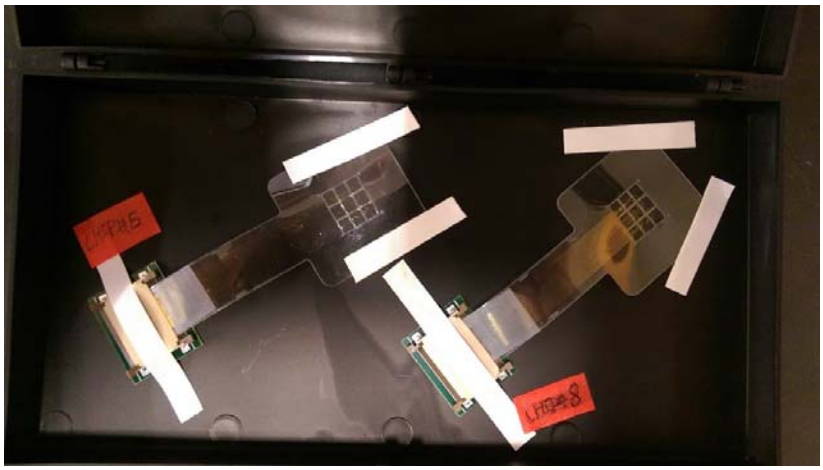

Figure 8. Copper tape-secured SiNW nanoFET meshes after assembly in an anti-static container before shipping.

<u>Objective 4.</u> Development of chemical functionalization of nanoFET mesh for specific antigen detection, and testing and characterization of the functionalized meshes

Antibody and PEG co-modification protocol development. To overcome Debye screening for selective biosensing in physiological environments, a mesh co-modification strategy with antibody and polyethylene glycol (PEG) was developed and optimized. We tested two modification strategies as follows, using 70 kDa dextran as an appropriately sized and charged VEEV analogue:

Method 1

1) APTES modification [1% APTES in (95% EtOH, 5% DI water) for 20 min]
2) Succinic anhydride modification [0.1 M succinic anhydride in DMF for 24 hr.]
3) Activation of carboxyl group by EDC/NHS [(2 mM/5 mM) in 1x PBS, micro fluidic channel.]
4) Injection of anti-dextran antibody and PEG-NH_2 (ratio = 1:2) [2 hr in 1x PBS, micro fluidic channel.]

Method 2

1) APTES modification [1% APTES in (95% EtOH, 5% DI water) for 20 min]
2) Glutaraldehyde modification [2.5% in DI water, for 2 hr]
3) Coupling anti-dextran antibody and PEG-NH_2 (ratio = 1:2) with sodium cyanoborohydride (5 mM) [in 1x PBS, micro fluidic channel for 2 hr.]

After modification by either method, samples were rinsed with fresh 1X PBS for 20 minutes. Rinsing was followed by injection of 10 μM 70 kDa dextran at a flow rate of 0.3 mL/hr for one hour to confirm specific binding of fluorescently-labeled antibody. Method 2 yielded reproducibly higher fluorescence intensity and uniformity than Method 1; tests of the method on bare Si wafers yielded the typical confocal fluorescence microscopy images shown below (**Figure 9**).

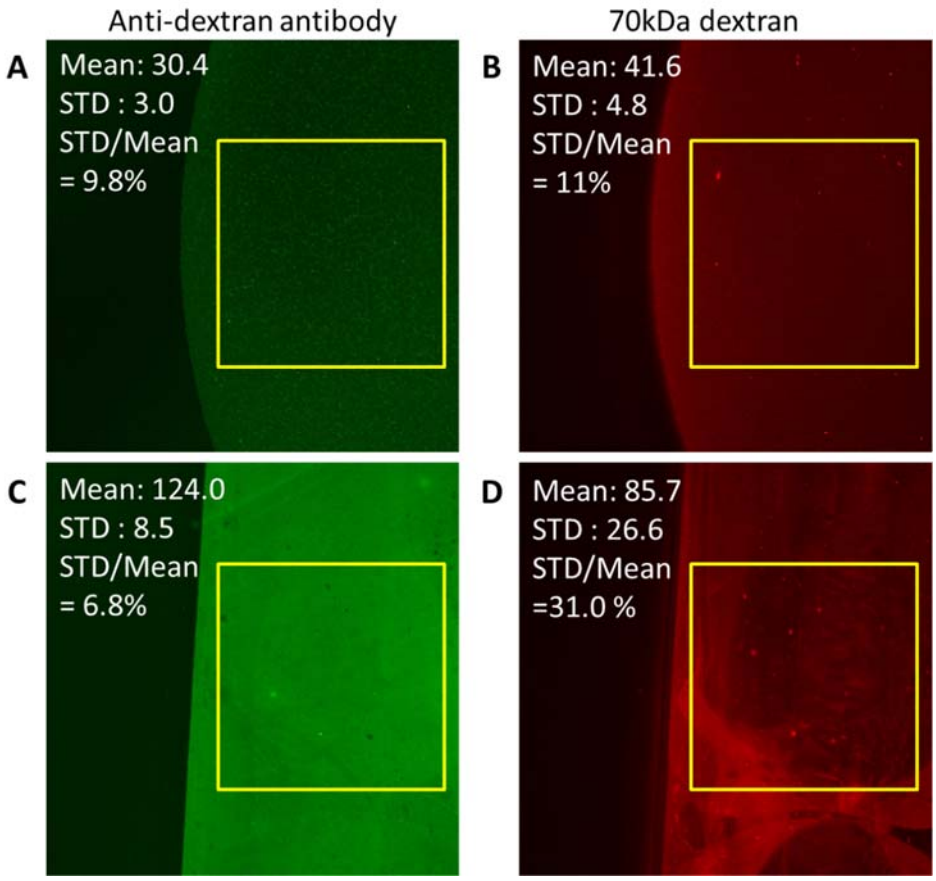

Figure 9. Confocal fluorescence microscopy images of Si wafer after anti-dextran antibody modification and 70 kDa dextran adsorption using Method 1 (**A, B**) and Method 2 (**C, D**).

Optimized antibody and PEG co-modification protocol for SiNW nanoFET mesh devices. Based on the initial results above, we developed the following glutaraldehyde-based co-modification protocol to prepare SiNW FETs for dextran sensing, which was shared with NRL personnel for their further use.

Anti-dextran and PEG co-modification protocol for SiNW FETs:

Chemical/reagent list

1. (3-Aminopropyl)triethoxysilane (APTES), 99%, Sigma-Aldrich (Product Number: 440140)
2. Glutaraldehyde, Grade I, 50% in water, Sigma-Aldrich (Product Number: G7651)
3. Anti-dextran antibody, Clone DX1, FITC, STEMCELL Technologies (Product Number: 60026FI)
4. Amino polyethylene glycol, mPEG-NH_2, MW = 40 kDa, Nanocs (Cat. Number: PG1-AM-40k)
5. Rhodamine B isothiocyanate dextran, MW = 70 kDa, Sigma-Aldrich (Product Number: R9379)
6. Sodium cyanoborohydride, reagent grade, 95%, Sigma-Aldrich (Product Number: 156159)

Solvent/Buffer solution list

1. Deionized water (Millipore DI water)
2. Ethanol (anhydrous)
3. 1X phosphate-buffered saline (1X PBS)

Detailed protocol

1) Subject SiNW mesh devices to oxygen plasma treatment, using 50W power with 50 sccm oxygen flow for 30 s.

2) Prepare a 90% by volume solution of ethanol with DI water and add 1% by volume APTES to the solution. Mix the solution and wait 20 minutes.

3) Immerse mesh devices in APTES solution for 20 min. Rinse the mesh with fresh ethanol gently 3 times. Dry the mesh in vacuum at room temperature for 1 hour.

4) Immerse the dried mesh into DI water for one hour. Carefully rinse the mesh with fresh DI water three times. Dry the mesh at room temperature.

5) Prepare 5% glutaraldehyde solution with 50% glutaraldehyde and DI water. Immerse the mesh device into glutaraldehyde solution for one hour. Rinse the mesh with fresh DI water gently three times.

6) Prepare modification solution: Dissolve in 800 μL 1X PBS (a) 0.466 μg mPEG-NH_2, (b) 1 μg Anti-dextran antibody and (c) 5 mM sodium cyanoborohydride.

7) Drop modification solution onto the mesh device region and make sure all FETs have good contact with the solution. Wait for two hours, until completion of the coupling reaction.

8) Rinse mesh with fresh 1X PBS three times. Take care to keep the antibody/PEG modified mesh devices from drying out.

Objective 5. Development of sensing strategy for specific detection of VEEV analogue dextran and VEEV-like particles in physiological solutions

Specific detection of VEEV analogue dextran in physiological solution using on-chip SiNW FET. To investigate the feasibility of VEEV-specific detection in physiological solutions, we successfully demonstrated that co-modification of on-chip SiNW FET with antibody and PEG enabled specific detection of dextran, a VEEV analogue, in 1X PBS.

As shown in **Figure 10B**, we carried out dextran-sensing control experiments in 1X PBS using unmodified, APTES-modified and antibody-modified SiNW FET. The results show no significant adsorption/binding curves, eliminating the possibility of interference from nonspecific dextran binding. In comparison with control experiments, PEG and antibody co-modified sensors clearly present irreversible dextran adsorption, where PEG modification serves as a buffer layer to overcome Debye screening in 1X PBS. It is worth noting that the sensing amplitude of 10 μM dextran varies with different co-modification ratios, as shown in **Figure 10C**.

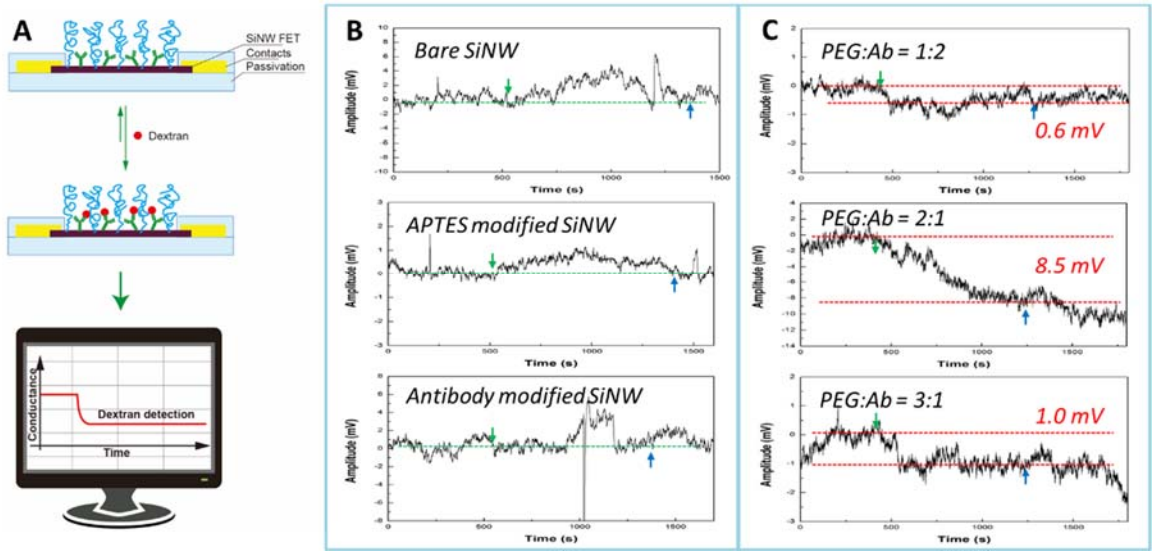

Figure 10. Dextran sensing in 1X PBS. **(A)** Schematic of dextran detection on antibody and PEG co-modified SiNW FET sensor. **(B)** Dextran sensing control experiments on unmodified, APTES- and antibody-modified SiNW FET sensors. **(C)** Dextran sensing experiments on PEG and antibody co-modified SiNW sensor, with 1:2, 2:1 and 3:1 PEG:antibody ratios. Green and blue arrows indicate introduction of 10 μM dextran and fresh 1X PBS.

To optimize the PEG and antibody modification ratio for maximum dextran sensing amplitude, various co-modification ratios were tested. The histogram in **Figure 11** summarizes dextran sensing performance versus co-modification ratio, suggesting 2:1 (PEG:antibody) outperformed all other ratios.

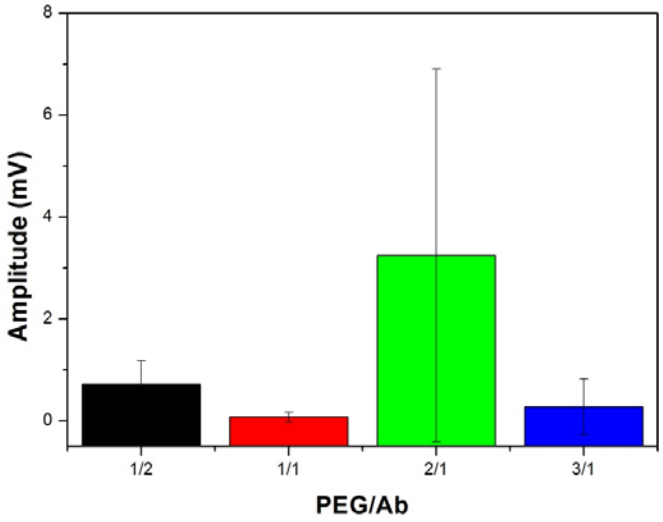

Figure 11. Histogram of 10 μM dextran sensing amplitude in 1X PBS on SiNW FET sensors with different PEG:antibody modification ratios.

Based on these results, we concluded the optimal PEG/antibody modification ratio for specific detection of the VEEV analogue dextran in physiological solution is near 2:1.

Specific detection of VEEV-like particles in physiological solution using on-chip SiNW FET. Based on our experience with detection of the VEEV analogue dextran in physiological solution, we carried out systematic sensing experiments to successfully demonstrate VEEV-specific detection using on-chip SiNW FET sensors with the above-described PEG/antibody co-modification protocol, and anti-VEEV antibody (Millipore Sigma, MAB8755, tested by USAMRIID). VEEV-like particles (VLP) are produced by transfecting cells with plasmids that encode only viral proteins. These proteins self-assemble and bud from the cells, and while they contain no genomic material and are therefore non-infectious, they are phenotypically similar to virus particles. VLP were supplied by Dr. Michael Lindquist at USAMRIID.

As with dextran sensing experiments, the device chip was rinsed thoroughly with 1X PBS to remove nonspecifically bound VEEV particles. False-color scanning electron microscopy (SEM) images in **Figure 12** clearly show VEEV particles bound to PEG/antibody modified SiNW.

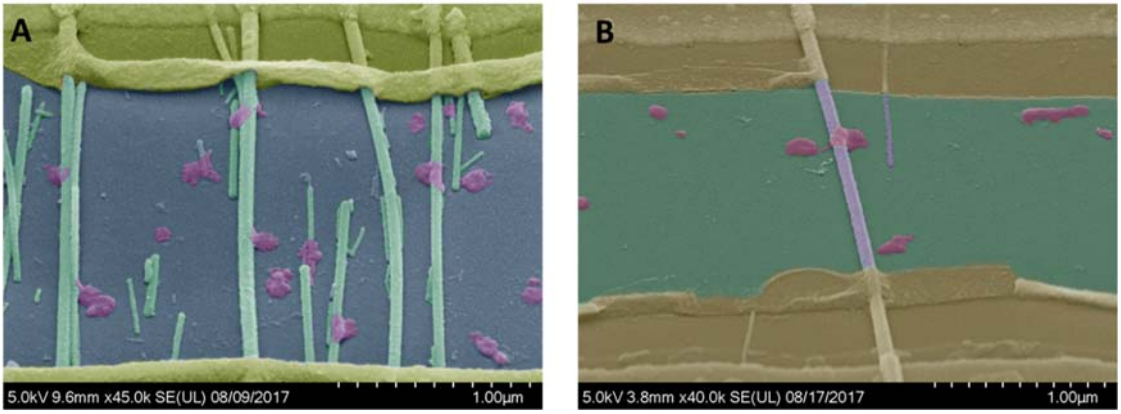

Figure 12. False-color scanning electron microscope (SEM) images of VLP binding to multiple **(A)** and single **(B)** SiNW FET sensors, where VLPs are shown in purple.

Consistent with the SEM images, actual sensing curves (**Figure 13**) of VLP on PEG/antibody co-modified SiNW FET sensors exhibit stepwise irreversible and pulse-like adsorption features. The stepwise or pulse adsorption nature of the curve was attributed to individual binding/unbinding events between VLP and anti-VEEV antibody.

Similarly, extensive sensing assays were performed to determine the optimal PEG:antibody modification ratio to maximize sensing step amplitude. As presented in the box chart from **Figure 14,** the optimal ratio is close to 1:1, with a maximum step amplitude of 2.6 mV. The step amplitude was found to be independent of viral load, in agreement with our hypothesis on the occurrence of individual VEEV binding/unbinding events.

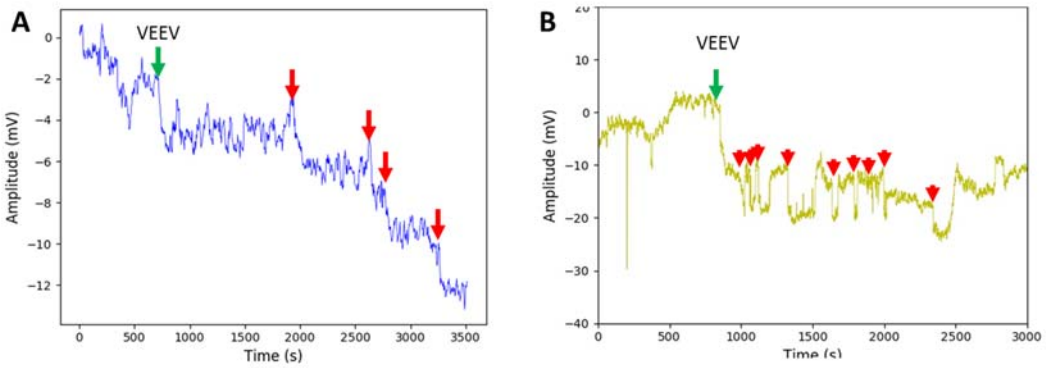

Figure 13. Typical VEEV sensing curves showing **(A)** stepwise irreversible adsorption and **(B)** reversible pulse like adsorption. Green and red arrows show times of VLP introduction.

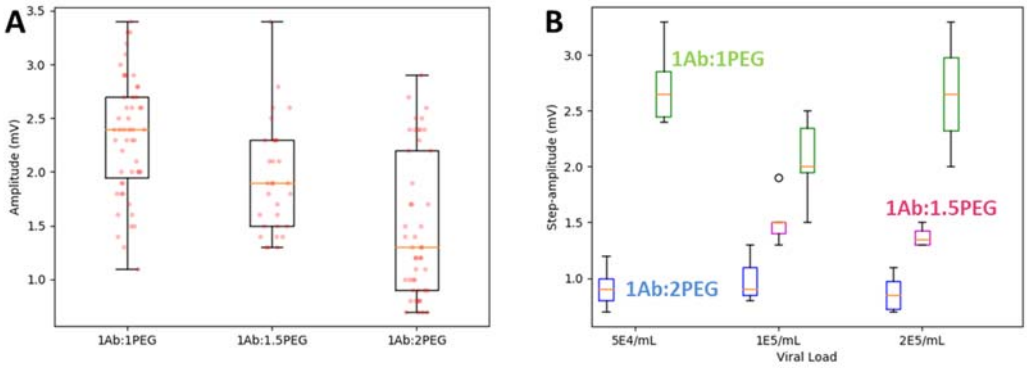

Figure 14. Box charts of sensing step amplitudes with different **(A)** co-modification ratio and **(B)** viral load.